International Journal of Solids and Structures 47 (2010) 2733–2744

Contents lists available at ScienceDirect

International Journal of Solids and Structures

journal homepage: www.elsevier.com/locate/ijsolstr

Modelling and transient planar dynamics of suspended cables with moving mass

Lianhua Wang [a,b], Giuseppe Rega [c,*]

[a] College of Civil Engineering, Hunan University, Changsha, Hunan 410082, PR China
[b] Key Laboratory of Building Safety and Energy Efficiency, Ministry of Education, Hunan 410082, PR China
[c] Department of Structural and Geotechnical Engineering, University of Rome 'La Sapienza', via A. Gramsci 53, Rome 00197, Italy

ARTICLE INFO

Article history:
Received 11 January 2010
Received in revised form 11 May 2010
Available online 4 June 2010

Keywords:
Suspended cable
3D modelling
Moving mass
Transient response
Parametric analysis
Horizontal tension

ABSTRACT

In this study, the 3D nonlinear equations of motion of the suspended cable with moving mass are obtained via the Hamilton principle, and its transient linear planar dynamics is investigated. Considering the quasi-static assumption, the condensed planar model accounting for the effect of the moving mass is derived, and it is then discretized by choosing the static deflection and sine series as shape functions. It is shown that this expansion shows good convergence features. The Newmark method is used to investigate the transient response. The effects of the inertia force, mass, sag and velocity of the moving mass on the transient dynamics of the suspended cable are systematically investigated. Finally, the horizontal tension of the suspended cable and the case of sequentially moving masses are examined.

1. Introduction

Cable structures play an important role in many engineering fields, such as civil, ocean and electrical engineering, and they are finding increased use in a wide variety of structural applications. Therefore, it is of interest to investigate the dynamics of suspended cables and cable structures. In recent years, numerous journal articles have addressed the nonlinear dynamics of bare suspended cables, see e.g., the review papers by Rega (2004). In addition, consideration of attached masses (Cheng and Perkins, 1992a,b; Al-Qassab and Nair, 2004) makes the treatment more involved due to the ensuing singularities in the deformed cable profile.

On the other hand, the moving load (mass) problem of distributed parameter systems is a very important topic in structural dynamics, and the response of structures subjected to a moving load (mass) is of considerable practical importance in different engineering fields. In this respect, Frýba (1999) presented various kinds of problems dealing with moving loads. More recently, lots of studies have focused on the dynamics of basic structural elements subjected to the moving load (mass), such as the beam (Thambiratnam and Zhuge, 1996; Michaltsos and Kounadis, 2001), arch (curved beam) (Yang et al., 2001; Wu and Chiang, 2004), plate (Kim and Roesset, 1998; Huang and Thambiratnam, 2002; Zhu and Law, 2003), and string (Gavrilov, 1999; Metrikine, 2004).

In contrast, only few studies have focused on the dynamics of the suspended cable with moving mass. Wu and Chen (1989) applied the finite element method (FEM) to investigate the dynamics of the suspended cable subjected to a moving load. Wang (2000) used the Galerkin method and Runge–Kutta method to examine the motion of an inclined cable with an accelerating mass. Al-Qassab et al. (2003) derived the equations of motions of horizontal and inclined cables with arbitrary sag and variable velocity of the moving mass. They also applied the classical Galerkin method and the wavelet-Galerkin method to discuss the dynamic behavior of the cable due to the moving mass along its length. Sofi and Muscolino (2007) derived the equations governing the planar motion of the coupled cable-moving oscillators system, and investigated the vibration of a shallow suspended cable carrying an array of moving masses with arbitrarily varying velocities. They treated the interaction force between the oscillators and the cable as a vertical external load entering the integro-differential equation of motion of the classical condensed model of the bare cable (Luongo et al., 1984). Overall, there is need: (i) to pursue a more general 3D formulation of the cable-moving mass problem, (ii) to account more exhaustively for the contribution to system dynamics of the inertia term of the moving mass and of other effects (influence of cable initial deflection, friction at the interface between cable and moving mass), (iii) to perform more parametric analyses aimed at understanding the system dynamic behavior.

In this study, the 3D dynamic model of the suspended cable subjected to a moving mass is developed based on a variational

* Corresponding author. Tel.: +39 06 49919195; fax: +39 06 3221449.
E-mail addresses: lhwang@hnu.cn (L. Wang), giuseppe.rega@uniroma1.it (G. Rega).

0020-7683/$ - see front matter © 2010 Elsevier Ltd. All rights reserved.
doi:10.1016/j.ijsolstr.2010.06.002

formulation (also used in Al-Qassab et al. (2003)), and the moving mass is assumed to move along the cable with either constant or variable velocity. A condensed planar model accounting for the effects of the moving mass on the cable dynamic tension is obtained and then discretized via the Galerkin expansion for linear dynamics. The Newmark method is applied to obtain the transient response of the cable. Systematic numerical analyses are performed to investigate the effects of some main parameters on the transient response. Moreover, the case of a suspended cable subjected to a sequence of moving masses is considered. The paper is organized as follows. In Section 2, the motion equations of the suspended cable with moving mass are obtained via the extended Hamilton principle. In Section 3, the improved condensed model of suspended cable with moving mass, based on the quasi-static assumption, is derived to investigate the transient planar dynamics. The model is discretized by the Galerkin method in Section 4, and the Newmark method used to obtain the transient response is summarized in Section 5. Section 6 presents extended numerical investigations of the transient response of the suspended cable subjected to moving mass, paying attention also to the evaluation of the dynamic tension. A short summary of results is presented in Section 7.

2. The continuum model

In this study, attention is focused on a suspended homogeneous elastic cable with span l, sag b and fixed ends, subjected to a moving mass M. A Cartesian coordinate system $O-xyz$ is chosen, with the origin O placed at the left support of the suspended cable. The static (dashed line) and non-planar dynamic (solid line) configurations of the suspended cable are shown in Fig. 1. The displacements of the point are denoted by $u(s,t)$, $v(s,t)$ and $w(s,t)$ along the x, y and z directions, respectively. Referring to the initial static equilibrium configuration and assuming the engineering strain as strain measure, the elongation of the cable element can be written as

$$\varepsilon(s,t)=\sqrt{(x'+u')^2+(y'+v')^2+w'^2}-1, \tag{1}$$

where the prime indicates differentiation with respect to the arc-length s.

2.1. Velocity of the moving mass

For the time t, the position vector of the cable point and its derivatives can be written as

$$\begin{aligned}\mathbf{r}&=[x(s)+u(s,t)]\mathbf{i}+[y(s)+v(s,t)]\mathbf{j}+w(s,t)\mathbf{k},\\ \mathbf{r}'&=[x'(s)+u'(s,t)]\mathbf{i}+[y'(s)+v'(s,t)]\mathbf{j}+w'(s,t)\mathbf{k},\\ \dot{\mathbf{r}}&=\dot{u}(s,t)\mathbf{i}+\dot{v}(s,t)\mathbf{j}+\dot{w}(s,t)\mathbf{k},\end{aligned} \tag{2}$$

where a dot indicates differentiation with respect to time t; $\mathbf{i}$, $\mathbf{j}$ and $\mathbf{k}$ are the unit vectors along the x, y and z directions, respectively. If we assume that the mass has a local scalar velocity $\dot{s}$, the velocity vector of the mass can be expressed by

$$\begin{aligned}\mathbf{V}_M&=\dot{\mathbf{r}}_M=(\dot{\mathbf{r}}+\mathbf{r}'\dot{s})|_{\mathbf{r}=\mathbf{r}_0,s=s_0}\\ &=\{[\dot{u}+\dot{s}(x'+u')]\mathbf{i}+[\dot{v}+\dot{s}(y'+v')]\mathbf{j}+[\dot{w}+\dot{s}w']\mathbf{k}\}|_{s=s_0},\end{aligned} \tag{3}$$

where $\mathbf{r}_0$, s_0 denote the current (i.e., at time t) position of the moving mass.

2.2. Variational formulation

The motion equations and corresponding boundary conditions of the suspended cable with moving mass can be obtained by using the extended Hamilton's principle, which may be expressed as:

$$\delta\int_{t_1}^{t_2}(T-U)\mathrm{d}t+\int_{t_1}^{t_2}\delta W\,\mathrm{d}t=0, \tag{4}$$

where T is the kinetic energy of the suspended cable and the moving mass; U is the strain energy of the suspended cable; δW is the sum of the variation of the potential energy and of the virtual work of non-conservative forces; and δ is the first variation.

The strain energy of the suspended cable can be expressed as

$$U=U^{(I)}+\int_0^{l_c}\left(T^{(I)}\varepsilon+\frac{1}{2}EA\varepsilon^2\right)\mathrm{d}s, \tag{5}$$

where $U^{(I)}$ and $T^{(I)}$ are respectively the strain energy and the cable tension of the initial configuration; l_c is the cable length; E is the modulus of elasticity; A is the cross-sectional area of the suspended cable.

The kinetic energy includes the kinetic energy of the suspended cable and the kinetic energy of the moving mass. Therefore, accounting for Eq. (3), it can be written as

$$\begin{aligned}T=&\frac{m}{2}\int_0^{l_c}(\dot{u}^2+\dot{v}^2+\dot{w}^2)\mathrm{d}s+\frac{M}{2}\int_0^{l_c}\delta(s-s_0)\big[\dot{u}^2+2\dot{u}\dot{s}(x'+u')\\ &+\dot{s}^2(x'+u')^2+\dot{v}^2+2\dot{v}\dot{s}(y'+v')+\dot{s}^2(y'+v')^2+\dot{w}^2\\ &+2\dot{w}\dot{s}w'+\dot{s}^2w'^2\big]\mathrm{d}s,\end{aligned} \tag{6}$$

where m is mass per unit length of the suspended cable; M is the mass of the moving mass; $\delta(\cdot)$ is the Dirac delta function.

The sum of the variation of the potential energy and of the virtual work of non-conservative forces can be written as

$$\begin{aligned}\delta W=&\int_0^{l_c}\{[-f(x'+u')\delta(s-s_0)-c_u\dot{u}]\delta u+[Mg\delta(s-s_0)+mg\\ &-f(y'+v')\delta(s-s_0)-c_v\dot{v}]\delta v-[fw'\delta(s-s_0)+c_w\dot{w}]\delta w\}\mathrm{d}s,\end{aligned} \tag{7}$$

where c_u, c_v and c_w are the viscous damping coefficients per unit length; g is the gravitational acceleration; and f is the friction force ($\mathbf{f}=f(x'+u')\mathbf{i}+f(y'+v')\mathbf{j}+fw'\mathbf{k}$) between the moving mass and the suspended cable (see the insert in Fig. 1)

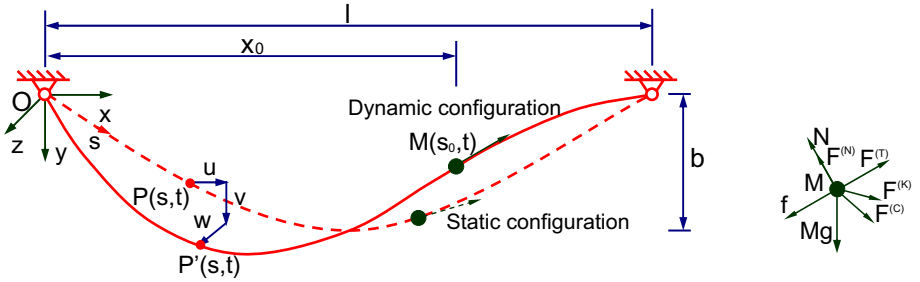

Fig. 1. The configurations of the suspended cable with moving mass.

$$f=\mu N,\quad N=-|\mathbf{F}^{(N)}|-Mg\cos\theta_M-|\mathbf{F}^{(C)}|\cos\theta_C-|\mathbf{F}^{(K)}|\cos\theta_K,$$
$$\theta_M=\arccos\left(\frac{Mg\mathbf{j}\cdot\mathbf{F}^{(N)}}{|Mg\mathbf{j}||\mathbf{F}^{(N)}|}\right);\quad \theta_C=\arccos\left(\frac{\mathbf{F}^{(C)}\cdot\mathbf{F}^{(N)}}{|\mathbf{F}^{(C)}||\mathbf{F}^{(N)}|}\right);$$
$$\theta_K=\arccos\left(\frac{\mathbf{F}^{(K)}\cdot\mathbf{F}^{(N)}}{|\mathbf{F}^{(K)}||\mathbf{F}^{(N)}|}\right). \tag{8}$$

In Eq. (8), μ is the friction coefficient; N is the reaction of the cable on the moving mass; $|\cdot|$ denotes absolute value; $\mathbf{F}^{(N)}$ is the centripetal force vector which arises due to the motion of the mass along the curved profile of the cable; $\mathbf{F}^{(K)}$ is the Coriolis force vector arising because the mass travels with velocity $\dot{s}$ in the longitudinal direction while the cable has angular velocity $\dot{\mathbf{r}}'$; $\mathbf{F}^{(C)}$ is the inertia force vector associated with the acceleration of the suspended cable. The expressions of the force vectors $\mathbf{F}^{(N)}$, $\mathbf{F}^{(K)}$ and $\mathbf{F}^{(C)}$ will be determined by the following analysis, along with that of the inertia force vector $\mathbf{F}^{(T)}$ due to the mass acceleration.

2.3. Equations of motion

Substituting the strain energy of Eq. (5), the kinetic energy of Eq. (6), and the variation of the potential energy plus the virtual work of non-conservative forces of Eq. (7) into Eq. (4), carrying out the conventional procedure of the calculus of variation, and assuming that $\delta u(s,t_1)=\delta u(s,t_2)=\delta v(s,t_1)=\delta v(s,t_2)=\delta w(s,t_1)=\delta w(s,t_2)=0$ (besides being $\delta u(0,t)=\delta u(l_c,t)=\delta v(0,t)=\delta v(l_c,t)=\delta w(0,t)=\delta w(l_c,t)=0$), we can obtain the equations of motions

$$m\ddot{u}+c_u\dot{u}-\left(\frac{(T^{(I)}+EA\varepsilon)(x'+u')}{\sqrt{(x'+u')^2+(y'+v')^2+w'^2}}\right)'=-\delta(s-s_0)[f(x'+u')]_{s=s_0}-M\delta(s-s_0)[\ddot{u}+2\dot{s}\dot{u}'+\dot{s}^2(x''+u'')+\ddot{s}(x'+u')]_{s=s_0}, \tag{9}$$

$$m\ddot{v}+c_v\dot{v}-\left(\frac{(T^{(I)}+EA\varepsilon)(y'+v')}{\sqrt{(x'+u')^2+(y'+v')^2+w'^2}}\right)'=-\delta(s-s_0)[f(y'+v')]_{s=s_0}+mg+Mg\delta(s-s_0)-M\delta(s-s_0)\left[\ddot{v}+2\dot{s}\dot{v}'+\dot{s}^2(y''+v'')+\ddot{s}(y'+v')\right]_{s=s_0}, \tag{10}$$

$$m\ddot{w}+c_w\dot{w}-\left(\frac{(T^{(I)}+EA\varepsilon)w'}{\sqrt{(x'+u')^2+(y'+v')^2+w'^2}}\right)'=-\delta(s-s_0)(fw')_{s=s_0}-M\delta(s-s_0)[\ddot{w}+2\dot{s}\dot{w}'+\dot{s}^2w''+\ddot{s}w']_{s=s_0}. \tag{11}$$

From Eqs. (9)–(11), we can see that the last part, in the right-hand side of each equation, accounts for the inertia force effects of the moving mass, and includes four terms: the first one is the inertia force due to the convected acceleration of the suspended cable: $\mathbf{F}^{(C)}=M\ddot{u}\mathbf{i}+M\ddot{v}\mathbf{j}+M\ddot{w}\mathbf{k}$; the second one is the inertia force due to the Coriolis acceleration: $\mathbf{F}^{(K)}=2M\dot{s}\dot{u}'\mathbf{i}+2M\dot{s}\dot{v}'\mathbf{j}+2M\dot{s}\dot{w}'\mathbf{k}$; the third one is the inertia force due to the centripetal acceleration: $\mathbf{F}^{(N)}=M\dot{s}^2(x''+u'')\mathbf{i}+M\dot{s}^2(y''+v'')\mathbf{j}+M\dot{s}^2w''\mathbf{k}$; the fourth one is the inertia force due to the mass relative acceleration: $\mathbf{F}^{(T)}=M\ddot{s}(x'+u')\mathbf{i}+M\ddot{s}(y'+v')\mathbf{j}+M\ddot{s}w'\mathbf{k}$. The boundary conditions can be written as

$$u(s,t)|_{s=0,s=l_c}=v(s,t)|_{s=0,s=l_c}=w(s,t)|_{s=0,s=l_c}=0. \tag{12}$$

The static equilibrium configuration of the bare cable can be obtained from Eqs. (9)–(11) by omitting the dynamic displacements terms, and the governing equations read

$$(T^{(I)}x')'=0,\quad (T^{(I)}y')'+mg=0,\quad 0\leqslant s\leqslant l_c, \tag{13}$$

with the solution being the extensible catenary.

3. Condensed planar model

For the shallow suspended cable, if the sag-to-span ratio is sufficiently small (i.e., $b/l<\frac{1}{8}$), the static configuration can be described accurately by a parabolic profile: $y(x)=4bx(l-x)/l^2$, which entails $\mathrm{d}s\approx\mathrm{d}x$ and $T^{(I)}\approx H$, where H is the horizontal component of the initial tension. Following Luongo et al. (1984), in order to investigate the planar dynamics of the shallow cable with moving mass, we can further assume the following hypotheses: (i) the gradient u' of the horizontal in-plane displacement component is negligible with respect to unity; and (ii) the initial strain is negligible with respect to unity ($H\ll EA$). Therefore, expanding the radical terms of Eqs. (9)–(11) in Taylor series up to the first order, which corresponds to express the extensional dynamic strain through its Lagrangian measure,

$$\varepsilon(x,t)=u'+y'v'+\frac{v'^2}{2}, \tag{14}$$

and considering the static equilibrium state, the planar dynamics of the suspended cable with moving mass is governed by the following approximate third-order nonlinear equations

$$m\ddot{u}+c_u\dot{u}-EA\left(u'+y'v'+\frac{v'^2}{2}\right)'=-\delta(x-x_0)f-M\delta(x-x_0)(\ddot{u}+2\dot{x}\dot{u}'+\dot{x}^2u''+\ddot{x})_{x=x_0}, \tag{15}$$

$$m\ddot{v}+c_v\dot{v}-\left[Hv'+EA(y'+v')\left(u'+y'v'+\frac{v'^2}{2}\right)\right]'=-\delta(x-x_0)[f(y'+v')]_{x=x_0}+Mg\delta(x-x_0)-M\delta(x-x_0)\left[\ddot{v}+2\dot{x}\dot{v}'+\dot{x}^2(y''+v'')+\ddot{x}(y'+v')\right]_{x=x_0}, \tag{16}$$

with the prime now denoting differentiation with respect to x. Eqs. (15) and (16) hold in the whole domain $x\in(0,l)$.

For the suspended cable with small sag, we can assume a quasi-static stretching during the cable motion. Under this assumption, the classical static condensation aimed at obtaining a sole integro-differential equation in the vertical displacement can be pursued, as in the bare cable (Luongo et al., 1984; Rega, 2004). To this aim, besides neglecting the acceleration and velocity terms as in the classical case, the centripetal terms are also omitted in Eq. (15), whereas the friction force and the inertia force due to the moving mass are included in order to account for the relevant effect on the system dynamics. It follows

$$\left(u'+y'v'+\frac{v'^2}{2}\right)'=\frac{M\ddot{x}_0+f}{EA}\delta(x-x_0). \tag{17}$$

Integrating Eq. (17) twice over the whole domain $x\in(0,l)$, with the boundary conditions $u(0,t)=u(l,t)=0$, and accounting for the strain discontinuity at the mass location x_0 via the Heaviside function defined as

$$H(x-x_0)=\begin{cases}0, & \text{for}\quad 0\leqslant x<x_0,\\ 1, & \text{for}\quad x_0\leqslant x\leqslant l,\end{cases} \tag{18}$$

we can obtain

$$u(x,t) = e(t)x - \int_0^x \left(y'v' + \frac{v'^2}{2}\right)\mathrm{d}x + \frac{M\ddot{x}_0 + f}{EA}(x - x_0)H(x - x_0), \tag{19}$$

where

$$e(t) = \frac{1}{l}\int_0^l \left(y'v' + \frac{v'^2}{2}\right)\mathrm{d}x - \frac{M\ddot{x}_0 + f}{EA \cdot l}(l - x_0). \tag{20}$$

Thus, the approximate dynamic strain ensuing from the integration of Eq. (17) reads

$$\begin{aligned}\varepsilon(x,t) &= \left(u' + y'v' + \frac{v'^2}{2}\right)\\ &= \frac{1}{l}\int_0^l \left(y'v' + \frac{v'^2}{2}\right)\mathrm{d}x - \frac{M\ddot{x}_0 + f}{EA \cdot l}(l - x_0) + \frac{M\ddot{x}_0 + f}{EA}H(x - x_0),\end{aligned} \tag{21}$$

and the integro–differential equation of transverse motion for the condensed planar cable model with moving mass can be written as

$$\begin{aligned}&m\ddot{v} + c_v\dot{v} - Hv'' - \frac{EA}{l}(y'' + v'')\left[\int_0^l \left(y'v' + \frac{v'^2}{2}\right)\mathrm{d}x - \frac{M\ddot{x}_0 + f}{EA}(l - x_0)\right.\\ &\left. + \frac{(M\ddot{x}_0 + f)l}{EA}H(x - x_0)\right] = Mg\delta(x - x_0)\\ &- M\delta(x - x_0)\left[\ddot{v} + 2\dot{x}\dot{v}' + \dot{x}^2(y'' + v'')\right]_{x=x_0}.\end{aligned} \tag{22}$$

Note that, of course, Eqs. (19)–(22) could also be obtained by integrating Eq. (17) in the two connected sub-domains of the cable, accounting for also the geometric $(u(x_0^+,t) = u(x_0^-,t))$ and mechanical $(H(x_0^+,t) - H(x_0^-,t) = M\ddot{x}_0)$ conditions at the mass location $x = x_0$ with $H(x,t) = EA\varepsilon(x,t)$ being the cable dynamic tension.

Compared with the *classical* condensed planar model used by Sofi and Muscolino (2007), some main differences occur in the expression (21) and in the condensed integro-differential equation of motion (22). The approximate dynamic strain exhibits two contributions due to the relative acceleration of the moving mass, which arise within the variational formulation of the equations of motion and ensue from retaining the inertia term of the moving mass and the friction in the condensation procedure. Both effects are neglected in the classical condensation, where the dynamic strain of the suspended cable turns out to be uniform along the cable span and is only a function of time t (Wang and Zhao, 2006; Srinil and Rega, 2007; Sofi and Muscolino, 2007). In contrast, in the present *improved* condensation, the strain (Eq. (21)) is a function of time t and of the mass location x_0 and friction and, owing to the Heaviside function dependent term, it is piecewise constant (namely, non-uniform) along the cable span. Of course, these contributions reflect themselves into the integro-differential equation of motion (22). Moreover, with respect to the companion equation based on classical condensation, Eq. (22) also contains the contribution of the initial configuration of the suspended cable to the centripetal acceleration $((\dot{x}^2y'')_{x=x_0})$, whereas the inertia force term due to the mass relative acceleration has disappeared from its right-hand side.

Overall, the present model accounting for the effect of the moving mass and the friction also in the condensation procedure might entail some differences in the system dynamic response with respect to the classical one, mostly as regards the space dependence of the dynamic tension.

4. Galerkin discretization

According to the Galerkin method, the transverse displacement $v(x,t)$ can be expressed in terms of the expansion:

$$v(x,t) = \sum_{j=1}^{N} q_j(t)\phi_j(x), \tag{23}$$

where $q_j(t)$ is the generalized displacement; $\phi_j(x)$ is a set of shape functions that satisfy the geometric boundary conditions: $\phi_j(0) = \phi_j(l) = 0$; N is the number of shape functions used in the approximation, which depends on the smoothness of the transverse displacement and the convergence of the series expression. Substituting Eq. (23) into Eq. (22), and simplifying, results in the following equation:

$$\begin{aligned}&m\sum_{j=1}^{N}\ddot{q}_j\phi_j + c_v\sum_{j=1}^{N}\dot{q}_j\phi_j - H\sum_{j=1}^{N}q_j\phi_j''\\ &\quad - \frac{EA}{l}\left(y'' + \sum_{j=1}^{N}q_j\phi_j''\right)\left[\int_0^l \left(y'\sum_{j=1}^{N}q_j\phi_j' + \frac{1}{2}\sum_{j=1}^{N}q_j\phi_j'\sum_{k=1}^{N}q_k\phi_k'\right)\mathrm{d}x\right.\\ &\quad \left. - \frac{M\ddot{x}_0 + f}{EA}(l - x_0) + \frac{(M\ddot{x}_0 + f)l}{EA}H(x - x_0)\right]\\ &\quad = Mg\delta(x - x_0) - M\delta(x - x_0)\left[\sum_{j=1}^{N}\ddot{q}_j\phi_j + 2\dot{x}\sum_{j=1}^{N}\dot{q}_j\phi_j'\right.\\ &\quad \left. + \dot{x}^2\left(y'' + \sum_{j=1}^{N}q_j\phi_j''\right)\right]_{x=x_0}.\end{aligned} \tag{24}$$

According to the Galerkin method, multiplying both sides of Eq. (24) by $\phi_i(x)$ and integrating over the span of the suspended cable, we can obtain a set of ordinary differential equations. If all nonlinear terms are neglected, the system of discretized equations governing the planar linear dynamics of the shallow suspended cable with moving mass can be written in the matrix form:

$$\mathbf{M}(t)\ddot{\mathbf{q}}(t) + \mathbf{C}(t)\dot{\mathbf{q}}(t) + \mathbf{K}(t)\mathbf{q}(t) = \mathbf{R}(t), \tag{25}$$

where $\mathbf{q} = \{q_1,\cdots,q_i,\cdots,q_N\}^T$ is the generalized displacement vector; $\mathbf{M}$ is the mass matrix; $\mathbf{K}$ is the stiffness matrix; $\mathbf{C}$ is the damping matrix; $\mathbf{R}$ is the load vector. $\mathbf{M}$, $\mathbf{C}$, $\mathbf{K}$ and $\mathbf{R}$ are all functions of the time t, and their elements read:

$$\begin{aligned}m_{ij} &= m\int_0^l \phi_j\phi_i\mathrm{d}x + M\phi_j(x_0)\phi_i(x_0);\\ c_{ij} &= c_v\int_0^l \phi_j\phi_i\mathrm{d}x + 2M\dot{x}_0\phi_j'(x_0)\phi_i(x_0);\\ k_{ij} &= H\int_0^l \phi_j'\phi_i'\mathrm{d}x + \frac{EA}{l}\int_0^l y''\phi_i\mathrm{d}x\int_0^l y''\phi_j\mathrm{d}x + \frac{(l - x_0)}{l}\\ &\quad \times\int_0^l (M\ddot{x}_0 + f)\phi_j''\phi_i\mathrm{d}x - \int_{x_0}^l (M\ddot{x}_0 + f)\phi_j''\phi_i\mathrm{d}x + M\dot{x}_0^2\phi_j''(x_0)\phi_i(x_0);\\ r_i &= Mg\phi_i(x_0) - \frac{(l - x_0)}{l}\int_0^l (M\ddot{x}_0 + f)y''\phi_i\mathrm{d}x\\ &\quad + \int_{x_0}^l (M\ddot{x}_0 + f)y''\phi_i\mathrm{d}x - M\phi_i(x_0)\dot{x}_0^2y''(x_0).\end{aligned} \tag{26}$$

It is worth noting how in Eq. (26), in addition to the standard terms of the bare suspended cable: (i) the mass matrix accounts for the convected acceleration term; (ii) the damping matrix for the Coriolis acceleration term; (iii) the stiffness matrix contains the centripetal term, as well as mass and friction dependent contributions from the dynamic strain; (iv) the load vector ensues from the moving mass and contains the friction and contributions to the terms at point (iii) accounting for the cable initial configuration.

4.1. The sine series

Although the natural modes of the suspended cable would be a good choice for the shape functions, to simplify the Galerkin procedure, a sine series may be used as assumed shape functions when enough number of terms are retained

$$\phi_j(x) = \sin\left(\frac{j\pi x}{l}\right), \qquad j = 1, \ldots, N. \tag{27}$$

4.2. The static deflection added sine series

However, the deformed shape of the cable, induced by the moving mass, cannot be described by a smooth continuous curve. This results in a very slow convergence of the sine series, as also observed in Al-Qassab et al. (2003), Sofi and Muscolino (2007), where the improvements obtainable with more sophisticated expansions were highlighted. In particular, the latter authors proposed to account for the pseudo-static contribution of the truncated high-frequency modes in the series expansion of the transverse displacement $v(x,t)$ (Eq.(23)) by adding to the modal series a correction term given by the difference of two different representations of the quasi-static solution. Yet, to the aim of this paper, the numerical results of Johnson et al. (2007) are of interest. They show that the introduction of a static deflection shape as an additional shape function can significantly improve the series convergence for the singularity problem of the deformed profile (see also Di Tomasso et al. (2003)). Therefore, this simple treatment is applied herein to investigate the transient dynamics of the suspended cable subjected to the moving mass. Considering the static deflection of a bare suspended cable due to a unit force at location $x = x_0$, the cable deflection is determined by the following equation

$$-Hv'' - \frac{EA}{l}\cdot y'' \int_0^l y'v'\mathrm{d}x = \delta(x - x_0), \tag{28}$$

whose solution can be written as

$$v(x) = \frac{3\lambda^2 x_0(l-x_0)}{Hl(12+\lambda^2)}\cdot\frac{x}{l}\cdot\left(\frac{x}{l}-1\right) + \frac{(l-x_0)x}{Hl} - \frac{(x-x_0)}{H}H(x-x_0), \tag{29}$$

where $\lambda^2 = 64EA/H\cdot(b/l)^2$ is the non-dimensional Irvine parameter (Irvine, 1981). If the maximum deflection of the suspended cable is normalized to unity, the static deflection shape function can be written as

$$\phi_1(x) = \frac{l^2(12+\lambda^2)}{l^2(12+\lambda^2) - 3\lambda^2(l-x_0)x_0} \times \left[\frac{3\lambda^2}{(12+\lambda^2)}\cdot\frac{x}{l}\cdot\left(\frac{x}{l}-1\right) + \frac{x}{x_0} - \frac{(x-x_0)l}{(l-x_0)x_0}H(x-x_0)\right], \tag{30}$$

with the other shape functions being assumed as sine functions as follows

$$\phi_j(x) = \sin\left(\frac{(j-1)\pi x}{l}\right), \quad j = 2, \ldots, N. \tag{31}$$

Note that a quasi-static assumption is also embedded in the deflection shape function $\phi_1(x)$, which is evaluated for fixed, though variable along the cable span, x_0 locations of the mass in the Galerkin discretization procedure. Of course, the actual $x_0(t)$ position of the moving mass will be correctly considered in the following numerical integration.

5. Numerical procedure

If we omit the effects of mass, the suspended cable will undergo free vibrations. In this case, the general solution of the equations of motion can be considered of the form: $\mathbf{q}(t) = \bar{\mathbf{q}}e^{i\omega t}$, where ω denotes the natural frequency of the suspended cable; $\bar{\mathbf{q}}$ is the modal vector; and $i = \sqrt{-1}$. Substitution of this form into Eq. (25) results in the following generalized eigenvalue problem

$$(\mathbf{K} - \omega^2\mathbf{M})\cdot\bar{\mathbf{q}} = \mathbf{0}. \tag{32}$$

By solving the eigenvalues of Eq. (32), we can obtain the natural frequencies of the suspended cable. For the case of the transient response analysis, the Newmark method has been proved to be convergent and unconditionally stable for a suitable choice of the parameters. Based on the classical Newmark method (Bathe, 1996), we can obtain the following equation for the time $t + \Delta t$

$$\left(\mathbf{K}_{t+\Delta t} + \frac{1}{\alpha\Delta t^2}\mathbf{M}_{t+\Delta t} + \frac{\beta}{\alpha\Delta t}\mathbf{C}_{t+\Delta t}\right)\cdot\mathbf{q}_{t+\Delta t} = \overline{\mathbf{R}}_{t+\Delta t}, \tag{33}$$

where Δt is the time step; $\alpha = \frac{1}{2}$ and $\beta = \frac{1}{4}$; and

$$\overline{\mathbf{R}}_{t+\Delta t} = \mathbf{R}_{t+\Delta t} + \mathbf{M}_t\left[\frac{1}{\alpha\Delta t^2}\mathbf{q}_t + \frac{1}{\alpha\Delta t}\dot{\mathbf{q}}_t + \left(\frac{1}{2\alpha}-1\right)\ddot{\mathbf{q}}_t\right] + \mathbf{C}_t\left[\frac{\beta}{\alpha\Delta t}\mathbf{q}_t + \left(\frac{\beta}{\alpha}-1\right)\dot{\mathbf{q}}_t + \left(\frac{\beta}{2\alpha}-1\right)\Delta t\ddot{\mathbf{q}}_t\right]. \tag{34}$$

After the displacement response $\mathbf{q}_{t+\Delta t}$ is determined, the acceleration and velocity responses can be obtained as follows:

$$\ddot{\mathbf{q}}_{t+\Delta t} = \frac{1}{\alpha\Delta t^2}(\mathbf{q}_{t+\Delta t} - \mathbf{q}_t) - \frac{1}{\alpha\Delta t}\dot{\mathbf{q}}_t - \left(\frac{1}{2\alpha}-1\right)\ddot{\mathbf{q}}_t, \tag{35}$$

$$\dot{\mathbf{q}}_{t+\Delta t} = \dot{\mathbf{q}}_t + \Delta t(1-\beta)\ddot{\mathbf{q}}_t + \beta\Delta t\ddot{\mathbf{q}}_{t+\Delta t}. \tag{36}$$

On the basis of the algorithm mentioned above, a *Mathematica* code has been developed in this study to determine the natural frequencies and the transient response of the suspended cable.

6. Numerical results and discussion

In this section, the method is used to investigate the transient planar linear dynamics of the suspended cable subjected to the moving mass, and to evaluate the effects of the centripetal and Coriolis force, of the sag-to-span ratio, and of the mass and velocity of the moving mass. In this study, the dimensional parameters and material properties of the suspended cable are as follows: the area of the cross-section $A = 1.175 \times 10^{-3}$ m^2, the mass per unit length of the cable $m = 9.7$ Kg/m, the Young modulus of the suspended cable $E = 147$ GPa, the cable span $l = 500$ m, the sag of the cable $b = 15$ m. Except for the sag b, the material properties and dimensions of the suspended cable are chosen to be identical to those of Sofi and Muscolino (2007).

Table 1 shows the rate of convergence of the first eight natural frequencies of the suspended bare cable. To compare with the calculated values, the natural frequencies obtained by the Irvine theory (Irvine, 1981) are also shown in Table 1. The natural frequencies are seen to converge fast with the number of sine terms, the converged values agreeing well with the analytical values obtained by the Irvine theory, and reasonably converged natural frequencies are obtained when $N = 32$.

Next, we consider that the mass is moving at constant velocity, $\dot{x}_0 = V$, starting from the left support of the suspended cable. Fig. 2 shows the midspan vertical displacement of the suspended cable for varying position of the moving mass with $V = 5$ m/s and $M = 100$ Kg. It is shown that the midspan displacement, obtained with 32 sine terms and with the static deflection added 3 sine terms, are almost coincident. It should be pointed out that these two curves are also close to the one obtained with 16 sine terms. Therefore, the use of 32 sine terms or of the static deflection added 3 sine terms is considered sufficient, and they are alternatively employed to investigate the dynamic response of the suspended cable subjected to the moving mass, in the remainder of this study. Furthermore, in the next subsections, in order to perform the parametric study of the cable with one moving mass, the viscous damping and the friction force are neglected. The first assumption can be considered acceptable given the low cable damping inher-

Table 1
The convergence study of the natural frequencies of the suspended cable.

N	ω_1	ω_2	ω_3	ω_4	ω_5	ω_6	ω_7	ω_8
2	1.79557	2.03261	–	–	–	–	–	–
4	1.79557	1.95176	2.81883	3.59114	–	–	–	–
8	1.79557	1.94537	2.81613	3.59114	4.50730	5.38671	6.29052	7.18228
16	1.79557	1.94461	2.81587	3.59114	4.50726	5.38671	6.29052	7.18228
32	1.79557	1.94451	2.81584	3.59114	4.50726	5.38671	6.29052	7.18228
Irvine theory (Irvine, 1981)	1.79557	1.94451	2.81584	3.59114	4.50726	5.38671	6.29052	7.18228

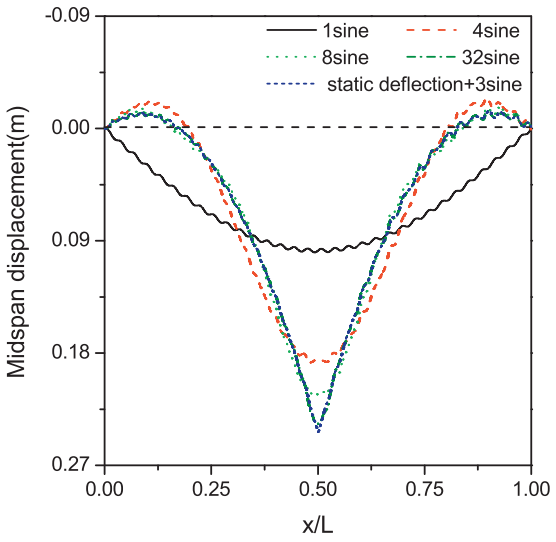

Fig. 2. The midspan vertical displacement of the suspended cable for varying position of the moving mass ($V = 5$ m/s, $f = 0.03$).

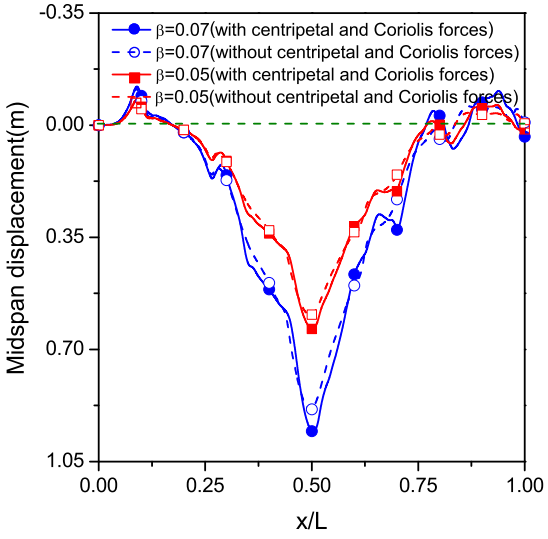

Fig. 3. Effects of the centripetal and Coriolis forces on the midspan vertical displacement of the suspended cable ($V = 25$ m/s, $f = 0.03$).

ent values and consideration of transient dynamics. Anyway, numerical results (not reported) show the substantially minor effect of damping on the time response also in a case of low velocity of the moving mass. In the parametric analysis, two non-dimensional parameters are used, the sag-to-span ratio $f = b/l$ and the mass ratio $\beta = M/ml$, with the relevant reference values being $f = 0.03$ and $\beta = 0.02$.

6.1. Effects of the centripetal and Coriolis forces

As stated in the Introduction, many studies focused on the moving load problem, where the inertia force of the mass was neglected. However, owing to large flexibility, relatively small mass and extremely low inherent damping of suspended cables, they are often susceptible to exhibit large amplitude vibration due to the moving mass (Al-Qassab et al., 2003; Sofi and Muscolino, 2007). In turn, the effects due to the interaction between the deflection of the suspended cable and the inertia force of the moving mass might further affect the dynamic behavior of the suspended cable. Herein, the full effect of the centripetal and Coriolis forces is systematically investigated. Fig. 3 shows the relevant effects on the midspan vertical displacement of the suspended cable with $V = 25$ m/s for two values of the mass ratio β. It is shown that, already for relatively large values of the mass ratio, the centripetal and Coriolis forces have some effect on the transient response of the suspended cable. Referring to Fig. 3, in the case of $\beta = 0.07$, the maximum midspan displacement of the suspended cable is 0.9290 m when the centripetal and Coriolis forces are included, whereas it is 0.8226 m when they are omitted.

Fig. 4 shows the effects of the centripetal and Coriolis forces on the maximum vertical displacement of the suspended cable with $V = 25$ m/s. In general, depending on the location along the cable, the effects of these forces are different. In the neighborhood of support ends, they can be neglected, as expectable. It is interesting to note that the involvement of the centripetal and Coriolis forces may also lead to the decrease of the maximum vertical displacement for some locations.

To gain a better understanding on the effects of the centripetal and Coriolis forces, Table 2 shows the comparison of maximum

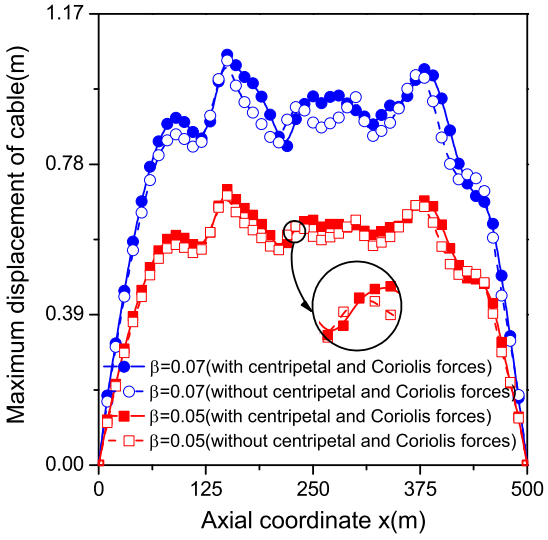

Fig. 4. The maximum vertical displacement of the suspended cable ($V = 25$ m/s, $f = 0.03$).

Table 2
The effects of the centripetal and Coriolis forces on the maximum midspan displacement of the cable.

		Maximum vertical midspan displacement (m)							
		With centripetal and Coriolis forces				Without centripetal and Coriolis forces			
β	f	5 m/s	10 m/s	20 m/s	40 m/s	5 m/s	10 m/s	20 m/s	40 m/s
0.0050	0.0025	0.01251	0.01235	0.01224	0.01227	0.01249	0.01229	0.01219	0.01226
	0.0050	0.02474	0.02518	0.02437	0.02290	0.02472	0.02516	0.02430	0.02261
	0.0100	0.04441	0.04604	0.04344	0.05091	0.04438	0.04597	0.04312	0.04960
	0.0200	0.05898	0.05894	0.05662	0.06728	0.05890	0.05868	0.05581	0.06383
0.0100	0.0025	0.02494	0.02465	0.02443	0.02459	0.02478	0.02464	0.02439	0.02445
	0.0050	0.04934	0.05037	0.04861	0.04589	0.04933	0.05032	0.04844	0.04531
	0.0100	0.08894	0.09199	0.08677	0.10174	0.08886	0.09186	0.08624	0.09934
	0.0200	0.11804	0.11760	0.11351	0.13472	0.11784	0.11738	0.11211	0.12848
0.0200	0.0025	0.04962	0.04918	0.04908	0.04940	0.04960	0.04913	0.04904	0.04913
	0.0050	0.09820	0.10181	0.09668	0.09213	0.09817	0.10069	0.09634	0.09110
	0.0100	0.17845	0.18335	0.17304	0.20309	0.17825	0.18324	0.17189	0.19823
	0.0200	0.23695	0.23480	0.22797	0.26966	0.23576	0.23282	0.22476	0.25871
0.0400	0.0025	0.09941	0.09911	0.09917	0.09968	0.09938	0.09901	0.09906	0.09927
	0.0050	0.19474	0.20113	0.19110	0.18593	0.19461	0.20104	0.19006	0.18380
	0.0100	0.35988	0.36373	0.34430	0.40422	0.35904	0.36248	0.34100	0.39678
	0.0200	0.47032	0.46210	0.45960	0.54062	0.46525	0.46067	0.45328	0.51454

midspan displacement as obtained for different mass ratios, sag-to-span ratios and velocity values. It is evident from Table 2 that the centripetal and Coriolis forces entail slightly greater values of the maximum midspan displacement, with the effects becoming more significant as the mass ratio and the sag-to-span ratio increase. In contrast, an increase of velocity with fixed β and f values does not necessarily entail an increase of the maximum midspan displacement of the cable, which can even decrease for some cases, as shown in Table 2. This might be due to the fact that the higher velocity leads to a shorter time for the midspan displacement to attain a large value than the lower velocity.

The present improved condensed model also accounts for the contribution of the cable initial configuration to the inertia force of the moving mass, contrary to the classical condensation. However, it should be pointed out that, with the relatively low values of sag-to-span ratio allowed by the cable shallowness assumption and with no mass acceleration and friction, the numerical results (not reported) show very small effects of the initial configuration contribution to the centripetal acceleration term in the expression of r_i (see Eq. (26)).

6.2. Effects of the sag-to-span ratio

The sag of the suspended cable plays an important role in its transient response under the moving mass. To illustrate the effects of the sag, the response of the suspended cable is evaluated for different values of the sag-to-span ratio f with $\beta = 0.02$ and $V = 10$ m/s. Fig. 5 shows the effects of the sag-to-span ratio on the maximum vertical displacement of the suspended cable. It is shown that the maximum deflection of the cable increases as the sag-to-span ratio increases, and exhibits large fluctuations along the cable (i.e., with respect to the axial coordinate x).

For a given sag-to-span ratio, these fluctuations increase (decrease) if the mass velocity increases (decreases). Using Eq. (29) to obtain the maximum static deflection ($x = x_0$), the curves in Fig. 5a (which is the static counterpart of Fig. 5b) are obtained, whose values occur at the corresponding coordinates in the horizontal axis when the fixed mass is located just at that point. Overall, consistent with the assumed Galerkin representation of the transverse displacement, the pattern of the maximum displacement diagram ensues from the superposition of the dynamic fluc-

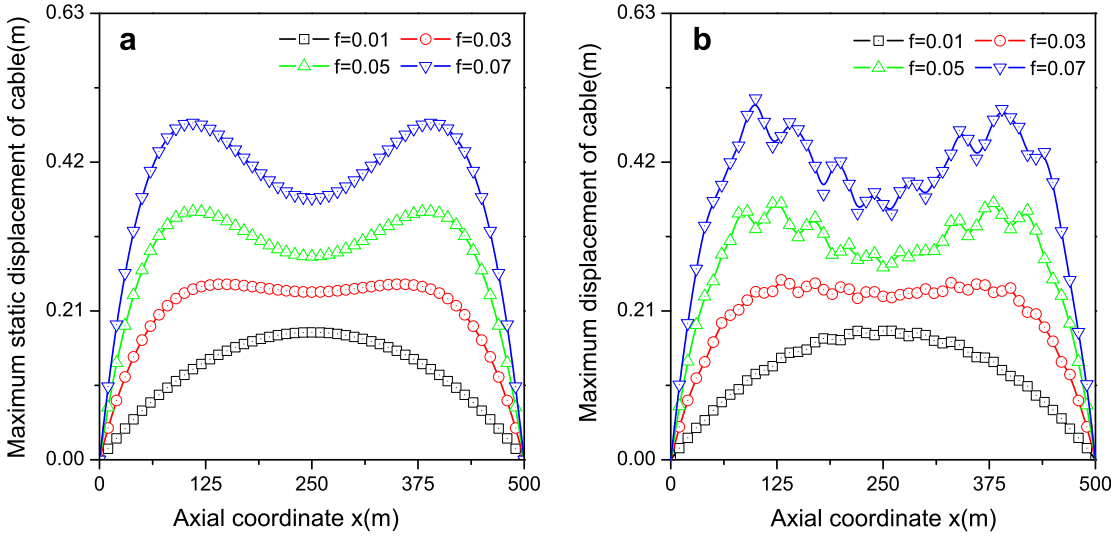

Fig. 5. Effects of the sag-to-span ratio on the maximum vertical displacement of the suspended cable ($V = 10$ m/s, $\beta = 0.02$): (a) static displacement; (b) dynamic displacement.

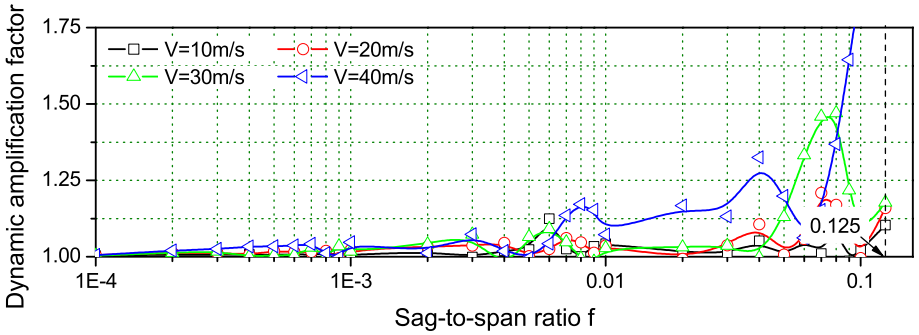

Fig. 6. The dynamic amplification factor of the midspan displacement of the suspended cable ($\beta = 0.01$).

tuations onto the maximum static deflection curve. Since the maximum dynamic deflection at a point does not always occur when the mass is located therein (e.g., the maximum deflection of the midspan does not occur when the mass is at midspan, see Section 6.4 forward), combining the two effects entails preserving the global symmetry of the dominant quasi-static response in the overall curve shape but losing the local one due to dynamic effects. The dynamic fluctuations could be due to a combination of traveling long- and short-length waves, arising for larger sag-to-span ratio or larger velocity.

In practice, the sag-to-span ratio of the suspended cable can be designed across a wide range of technical values. To seek their effects on the planar dynamics, the relationship between the dynamic amplification factor and the sag-to-span ratio is examined. The effects of the sag-to-span ratio on the dynamic amplification factor of the midspan displacement of the suspended cable with $\beta = 0.01$ are shown in Fig. 6, where the dynamic amplification factor is defined as

$$\phi = \frac{v_{d,max}}{v_{st}}, \tag{37}$$

where $v_{d,max}$ denotes the maximum dynamic deflection of a certain point of the suspended cable, and v_{st} denotes the static deflection of the same point of the cable with the fixed mass. It is shown that the dynamic amplification factors of the midspan deflection basically remain constant when the sag-to-span ratio is in the range $f \in (1.0 \times 10^{-4}, 1.0 \times 10^{-3})$ when $V < 40$ m/s, and the effects of the velocity of the moving mass on the dynamic amplification factor are quite insignificant. However, the influence of the sag-to-span ratio and velocity is significantly enhanced at higher values of the sag-to-span ratio f, as shown in Fig. 6. When the sag-to-span ratio increases up to about 0.005, significant differences among the factors are observed. Moreover, some visible peaks can be observed for the larger velocities. However, some uneasily understandable effects of increasing the velocity beyond a certain level, possibly due again to traveling wave contributions, are observed, along with variable effects of increasing the sag-to-span ratio up to values where the parabolic approximation might become questionable.

6.3. Effects of the mass of the moving mass

The mass of the moving mass determines the inertia force and dynamic interaction between the suspended cable and the mass. Therefore, it affects the dynamic response of the suspended cable, as already observed in Fig. 4. The effects of the mass of the moving mass on the maximum vertical displacement of the suspended cable with $V = 10$ m/s are shown in Fig. 7. As expected, an increase in the mass ratio results in an increased maximum displacement of the suspended cable. Obviously, with an increasing mass, the dynamic interaction between the cable and the moving mass becomes more

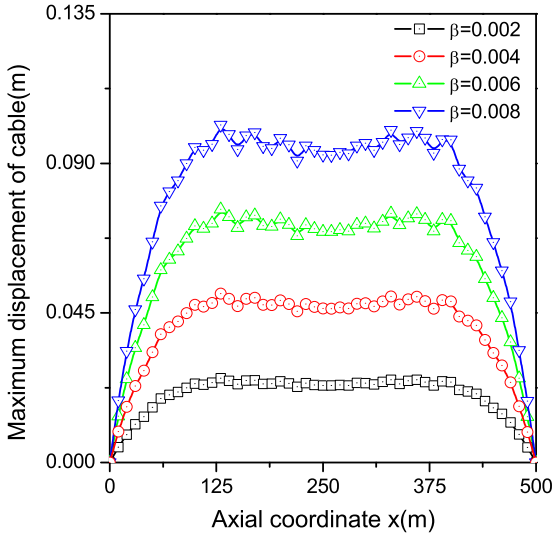

Fig. 7. Effects of the mass ratio on the maximum vertical displacement of the suspended cable ($V = 10$ m/s, $f = 0.03$).

important. Fig. 8 illustrates the dynamic amplification factors of the midspan displacement of the suspended cable with $f = 0.03$ for different mass velocities. It is shown that the values are nearly constant and the dynamic amplification factor curve when $V = 20$ m/s is nearly identical to the curve when $V = 30$ m/s, for low values of mass ratio β. It is interesting to note that the dynamic amplification factor when $V = 10$ m/s is larger than the one when $V = 20,30$ m/s for any mass ratio β, thus confirming an observation already made on the results in Table 2. For values of the mass ratio above 0.01, the dynamic amplification factor curves for different velocities exhibit different behaviors.

6.4. Effects of the velocity of the moving mass

The velocity of the moving mass plays an important role in the inertia force and dynamic interaction between the suspended cable and the mass. However, previous results show that the increase of the moving mass velocity may result in the decrease of the midspan displacement. To more clearly illustrate this unexpectable phenomena, the case $\beta = 0.035$ and $f = 0.045$ is carefully considered, and the velocity of the moving mass is varied from 1 to 70 m/s. Fig. 9 shows the effects on the dynamic deflection at the midspan of the suspended cable, highlighting a decrease of the maximum midspan displacement when the velocity of the moving mass increases. Moreover, for different velocities, this maximum midspan displacement occurs when the mass is at slightly different locations along the span. For the case of $V = 40$ m/s, the maximum

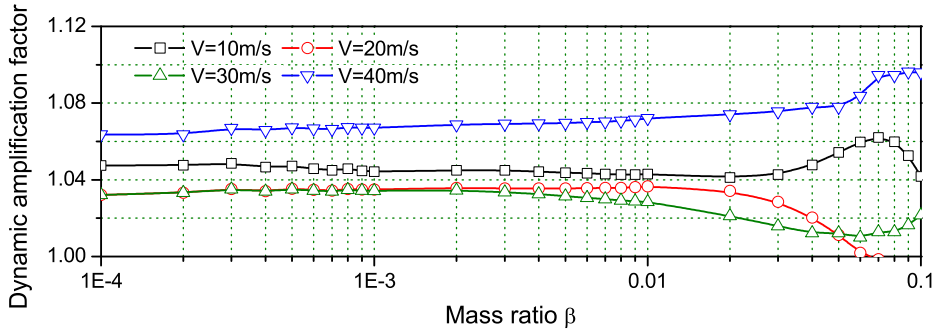

Fig. 8. The dynamic amplification factor of the midspan displacement of the suspended cable ($f = 0.03$).

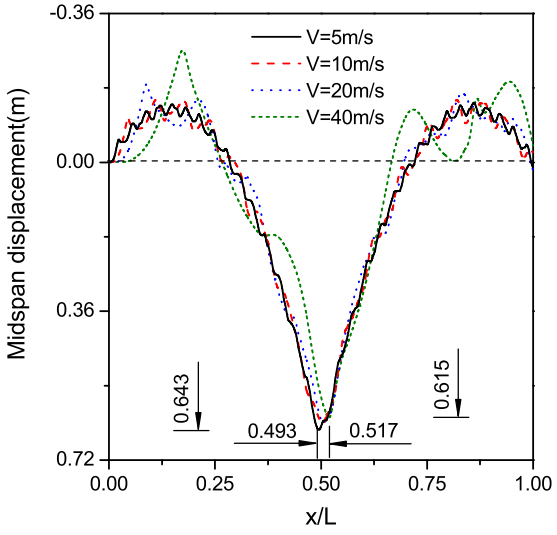

Fig. 9. The effects of the moving mass velocity on the midspan dynamic deflection ($\beta = 0.035$, $f = 0.045$).

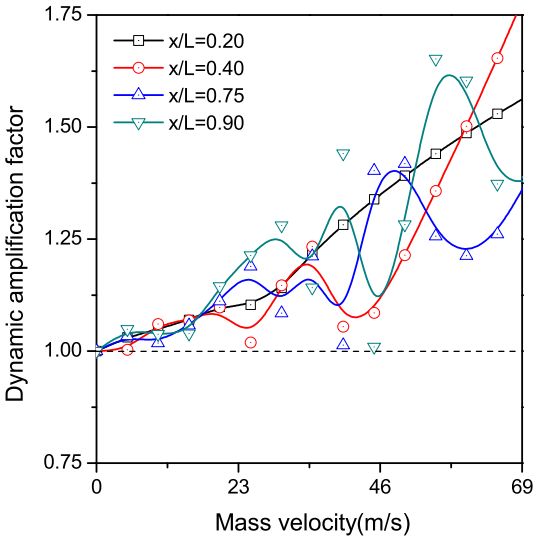

Fig. 10. The dynamic amplification factors at different locations of the suspended cable with varying mass velocity ($\beta = 0.02$, $f = 0.03$).

midspan displacement ($v_{max}(0.5L, 6.16\ s) = 0.615$ m) occurs when the mass is located at $x/L = 0.517$.

Different locations exhibit different maximum displacement values. Therefore, the dynamic amplification factors vary along the cable span. Fig. 10 shows the variation of the dynamic amplification factor at different locations of the suspended cable with the mass velocity varying in the range $V \in (1\ m/s, 70\ m/s)$. It is shown that the effect of the velocity of the mass on the dynamic amplification factor is small and nearly comparable at all locations when $5\ m/s \leqslant V \leqslant 20\ m/s$. Instead, for larger mass velocities, the dynamic amplification factors at different locations exhibit visible "resonance" phenomena, e.g., at 9/10 span when $V \approx 55$ m/s. This might be due to some kind of parametric resonance, as those discussed in Luongo and Piccardo (2009).

6.5. The response under varying velocity

Previous investigation mainly focused on the mass constant velocity. In fact, the mass may move along the suspended cable with variable velocity and acceleration. The motion of the mass can be described by an arbitrary function $x(t)$. As an example, we consider the following law (Sofi and Muscolino, 2007):

$$x(t) = \begin{cases} V_0 t, & \text{for} \quad t < t_0, \\ V_0 t_0 + V_0(t - t_0) + \frac{1}{2} a_0 (t - t_0)^2, & \text{for} \quad t \geqslant t_0, \end{cases} \tag{38}$$

where $V_0 = 5$ m/s, $t_0 = 90$ s and $a_0 = -0.25\ m/s^2$. For this case, the moving mass starts from the left support and moves with constant velocity $V = V_0$, until it reaches 9/10 span of the suspended cable. Then, it is subjected to a deceleration a_0, and stops at the right support at time $t = 110$ s. Fig. 11 shows the time history of the midspan vertical displacement of the suspended cable for different sag-to-span ratios. Of course, the maximum value is reached after 50 s, i.e., when the mass passes through the midspan. On the right side, it is shown that the inertia force, due to the deceleration of the moving mass, slightly changes the vibration form of the midspan deflection. Moreover, the effect of the sag-to-span ratio on this alteration is very small. Obviously, the deceleration of the moving mass slows down the midspan deflection decay. After the mass moves past the right support at time $t = 110$ s, the suspended cable undergoes free vibration, as shown in Fig. 11. It is interesting to note that the amplitude of the free vibration for the largest sag-to-span ratio value ($f = 0.06$) is considerably larger than for the other cases.

6.6. The horizontal tension of the suspended cable

In the engineering field, the tension of the suspended cable is a very important design factor. To investigate the tension of the suspended cable with moving mass, the total horizontal tension H_T is considered, defined as

$$\begin{aligned} H_T &= H + EA\varepsilon(x,t) \\ &= H + \frac{EA}{l}\sum_{j=1}^{N} q_j \int_0^l y'\phi_j' dx - \frac{M}{l}\ddot{x}_0(l - x_0) + M\ddot{x}_0 H(x - x_0), \end{aligned} \tag{39}$$

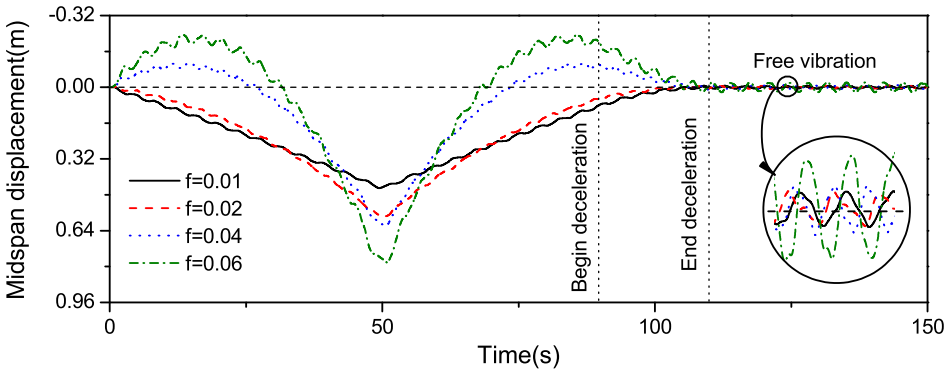

Fig. 11. Time history of the midspan vertical displacement of the suspended cable with variable mass velocity ($\beta = 0.05$).

where the last two terms in Eq. (39) originate from the relative acceleration of the moving mass, and the friction term is neglected. Accordingly, unlike the classical condensation procedure, in the case of varying velocity, the horizontal tension is also a time-dependent function of the mass location x_0, and, mostly, it is piecewise uniform along the cable span owing to the Heaviside function term included in Eq. (39). Obviously, the space-moving horizontal tension difference at $x_0^{\pm}$ is $|M\ddot{x}_0|$, as determined by the relative acceleration of the moving mass.

To illustrate the time- and space-varying effect of the inertia force on the horizontal tension of the suspended cable, we consider the case of the mass moving along the cable with varying velocity and different acceleration, the varying velocity law being assumed as

$$V(t) = \begin{cases} 4, & \text{for} \quad 0\ \text{s} \leqslant t < 12\ \text{s}, \\ 4 + 2(t-12), & \text{for} \quad 12\ \text{s} \leqslant t < 26\ \text{s}, \\ 32 - 4(t-26), & \text{for} \quad 26\ \text{s} \leqslant t < 32\ \text{s}, \\ 8, & \text{for} \quad 32\ \text{s} \leqslant t \leqslant 42\ \text{s}. \end{cases} \tag{40}$$

For this case, the moving mass starts from the left support and moves with a constant velocity $V = 4$ m/s at time $t = 0$ s, and it reaches the right support with another constant velocity $V = 8$ m/s at time $t = 42$ s. Moreover, it undergoes the acceleration and deceleration stages when it moves along the cable span. Since the expression of the horizontal tension includes the integral term, the 32 sine terms expansion is used in order to simplify the numerical integration. Fig. 12 shows the total horizontal tension diagrams along the cable span at different time instants with $\beta = 0.05$, $f = 0.06$ and the moving mass variable velocity. The total horizontal tension obtained through the classical condensation procedure is also illustrated in Fig. 12. At the time $t = 0$ s, no action of the mass occurs. In this case, the horizontal tensions, obtained by the improved and classical condensation procedure, are the same and are determined by the static configuration analysis, as shown in Fig. 12. When the mass moves along the cable span with a constant velocity, the sole minor tension difference between the two procedures ensues (i.e., at times $t = 5$ s and $t = 42$ s) from the small effects of the initial configuration of the suspended cable on the centripetal acceleration, taken into account in the improved condensation. However, the tension difference between the two condensed model becomes clearer when the mass undergoes the non-constant velocity, and the step phenomenon occurring at variable locations of the mass moving along the cable is observed. It entails a piecewise constant horizontal tension in the improved model. Since acceleration and deceleration values are considered, upward and downward horizontal tension steps are observed at $x_0^{\pm}$ in the tension diagram. Overall, looking at Fig. 12, the classical condensation procedure is seen to underestimate (possibly overestimate) the horizontal tension on the right (left) side of the moving mass location when the mass undergoes acceleration, and underestimate (possibly overestimate) it on the left (right) side when the mass undergoes deceleration. This turns out to be of some interest also from the design viewpoint, where the horizontal tension is a factor of major interest.

Another interesting issue is concerned with the difference of the dynamic displacements as obtained with the classical and improved condensed models. It is also illustrated in Fig. 12, which shows the midspan displacement of the suspended cable for varying position of the moving mass. Obviously, the midspan displacement difference is very small when the mass moves along the cable span with uniform velocity, as previously stated at the end of Section 6.1. In contrast, it is significantly enhanced (considering the scale of the vertical axis) in the acceleration and deceleration stages, where all of the mass-dependent terms retained in the discretization (Eq. (25)) of the improved model come into play.

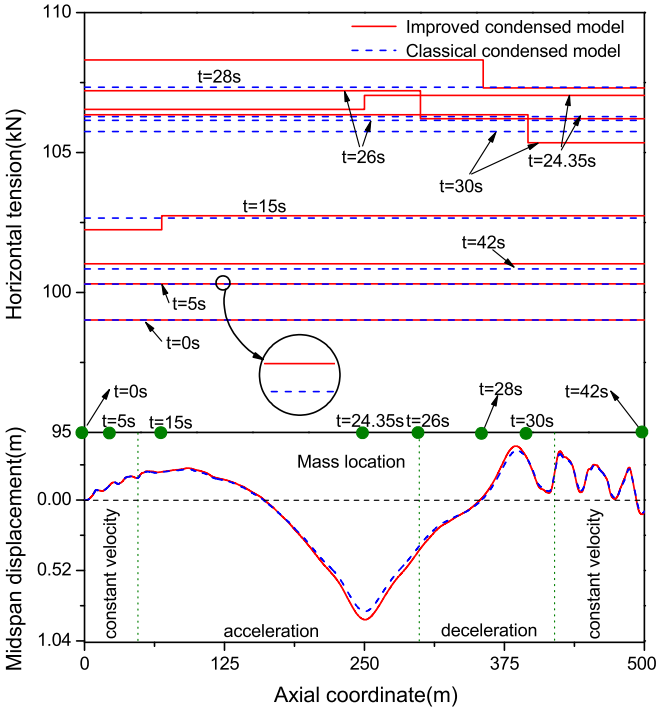

Fig. 12. Horizontal tension at different instants and midspan displacement of the suspended cable with varying mass velocity ($\beta = 0.05$, $f = 0.06$), for the improved and classical condensed models.

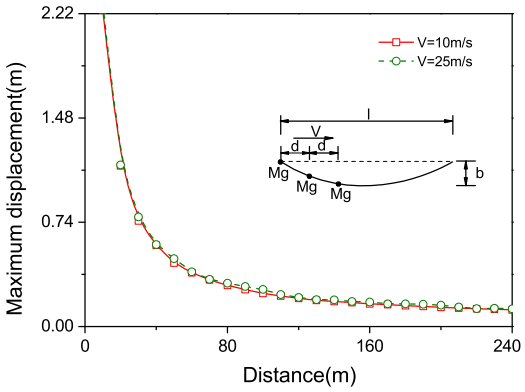

Fig. 13. Variation of maximum deflection at midspan of the suspended cable with the mass distance ($\beta = 0.01$, $f = 0.03$).

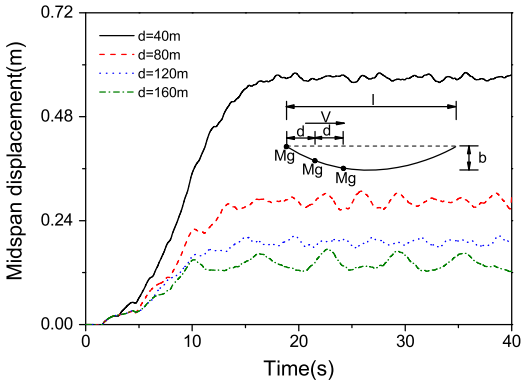

Fig. 14. The transient response of the midspan for different mass distances ($\beta = 0.01$, $f = 0.03$, $V = 25$ m/s).

6.7. The case of sequentially moving masses

In fact, the moving masses are often sequentially distributed along the cable. In this case, the distance between adjacent masses determines its dynamic response. Next, we consider a continuous stream of moving masses with same constant velocity, and the 32 sine terms approximation is still applied in this case. Fig. 13 shows the variation of the maximum deflection of the midspan of the suspended cable with the distance for the moving velocities $V = 10$ m/s and $V = 25$ m/s, where the distance d between adjacent masses is constant. Besides the obvious general decrease of the maximum midspan deflection with the increase of the distance d, it is seen from Fig. 13 that the former attains a nearly constant value with increase of the latter. It can also be seen that the velocity has only a minor effect on the maximum deflection for the case of continuously moving masses.

The transient responses of the midspan for different distances with a moving velocity $V = 25$ m/s are shown in Fig. 14. As expected, the maximum displacement decreases as the distance increases. However, the amplitude of the vibration around an average value increases as the distance increases. It is also interesting to note that for a relatively large number of masses, the deflection of the midspan still increases when the first mass moves past the midspan of the suspended cable ($t = 10$ s).

7. Conclusions

By applying the Hamilton principle, the 3D motion equations of the suspended cable subjected to moving mass and fully accounting for the relevant contributions have been presented in this study. Then, an improved condensed planar model, accounting for the effect of the moving mass on the extensional strain of a shallow cable, has been obtained. The static deflection and sine series have been chosen as shape functions to discretize the equations of motions, and the Newmark method has been used for the numerical integration. Systematic numerical results have been obtained to explore the transient planar linear dynamics of the suspended cable.

The effects of the centripetal and Coriolis forces on the response of the suspended cable have been investigated as well as those of the mass and velocity of the moving mass. It has been shown that the inertia forces of the moving mass enhance the maximum midspan displacement, and that the relevant effects play a more important role in the transient response when the mass of the moving mass increases. However, the increase of mass velocity may decrease the maximum displacement in a large range of mass ratio values.

Also the effects of the sag of the suspended cable have been investigated. The numerical results show that the maximum deflection of the cable increases as the sag increases. The time histories of the midspan displacement and horizontal tension of the suspended cable with the varying mass velocity have been examined. It has been shown that the classical condensation procedure cannot reflect the actual spatial dependence of the piecewise constant horizontal tension, ensuing from the presence of the moving mass, when the mass moves with non-uniform motion.

At last, the transient response of the suspended cable subjected to a sequence of masses moving with constant velocity has been studied. The numerical results show that the effects of the velocity on the maximum midspan displacement is very small.

Besides moving to a non-condensed model suitable for dealing with non-shallow cables, further studies based on the improved condensed model should focus on the evaluation of parameters and/or effects neglected in the present analysis (friction, sequence of moving masses with varying velocity) and on consideration of the nonlinear terms in the equations of motion.

Acknowledgement

The study was supported by National Science Foundation of China under Grant Nos. 10772065, 10972073 and NCET-09-0335. The first writer also acknowledges the financial support from the Hunan Science and Technology Project (No. 2008FJ3216) and the University of Rome 'La Sapienza'. Useful criticisms and suggestions from an anonymous reviewer are gratefully acknowledged.

References

Al-Qassab, M., Nair, S., 2004. Wavelet-Galerkin method for the free vibrations of an elastic cable carrying an attached mass. Journal of Sound and Vibration 270 (1–2), 191–206.
Al-Qassab, M., Nair, S., O'Leary, J., 2003. Dynamics of an elastic cable carrying a moving mass particle. Nonlinear Dynamics 33, 11–32.
Bathe, K.J., 1996. Finite Element Procedures. Prentice-Hall, New Jersey.
Cheng, S.P., Perkins, N.C., 1992a. Free vibration of a sagged cable supporting a discrete mass. Journal of the Acoustical Society of America 91 (5), 2654–2662.
Cheng, S.P., Perkins, N.C., 1992b. Closed-form vibration analysis of sagged cable/mass suspensions. ASME, Journal of Applied Mechanics 59, 923–928.
Di Tomasso, F., Di Egidio, A., Luongo, A., 2003. Modelling and dynamic analysis of strings carrying a single mass. In: Proc. of 16th AIMETA Congress, CD-Rom, Ferrara, Italy (in Italian).
Frýba, L., 1999. Vibration of Solids and Structures under Moving Loads. Thomas Telford, London.
Gavrilov, S., 1999. Non-stationary problems in dynamics of a string on an elastic foundation subjected to a moving load. Journal of Sound and Vibration 222, 345–361.
Huang, M.-H., Thambiratnam, D.P., 2002. Dynamic response of plates on elastic foundation to moving loads. ASCE, Journal of Engineering Mechanics 128, 1016–1022.

Irvine, H.M., 1981. Cable Structures. The MIT Press, Cambridge.
Johnson, E.A., Baker, G.A., Spencer Jr., B.F., Fujino, Y., 2007. Semiactive damping of stay cables. ASCE, Journal of Engineering Mechanics 133, 1–11.
Kim, S.M., Roesset, J.M., 1998. Moving loads on a plate on elastic foundation. ASCE, Journal of Engineering Mechanics 124 (9), 1010–1017.
Luongo, A., Piccardo, G., 2009. Perturbation and numerical analysis of suspended cables traveled by a single mass. In: Proc. of 19th AIMETA Congress, CD-Rom, Ancona, Italy.
Luongo, A., Rega, G., Vestroni, F., 1984. Planar nonlinear free vibrations of an elastic cable. International Journal of Nonlinear Mechanics 9 (1), 39–52.
Metrikine, A.V., 2004. Steady state response of an infinite string on a nonlinear visco-elastic foundation to moving point loads. Journal of Sound and Vibration 272, 1033–1046.
Michaltsos, G.T., Kounadis, A.N., 2001. The effects of centripetal and Coriolis forces on the dynamic response of light bridge under moving loads. Journal of Vibration and Control 7, 315–326.
Rega, G., 2004. Nonlinear vibrations of suspended cables. Part I: modeling and analysis, Part II: deterministic phenomena. Applied Mechanics Reviews 57, 443–478. 479–451.
Sofi, A., Muscolino, G., 2007. Dynamic analysis of suspended cables carrying moving oscillators. International Journal of Solids and Structures 44, 6725–6743.
Srinil, N., Rega, G., 2007. The effects of kinematic condensation on internally resonant forced vibrations of shallow horizontal cables. International Journal of Nonlinear Mechanics 42 (1), 180–195.
Thambiratnam, D., Zhuge, Y., 1996. Dynamic analysis of beams on an elastic foundation subjected to moving loads. Journal of Sound and Vibration 198, 149–169.
Wang, Y.M., 2000. The transient dynamics of a cable-mass system due to the motion of an attached accelerating mass. International Journal of Solids and Structures 37, 1361–1383.
Wang, L., Zhao, Y., 2006. Nonlinear interactions and chaotic dynamics of suspended cables with three-to-one internal resonances. International Journal of Solids and Structures 43, 7800–7819.
Wu, J.S., Chen, C.C., 1989. The dynamic analysis of a suspended cable due to a moving load. International Journal for Numerical Methods in Engineering 28, 2361–2381.
Wu, J.S., Chiang, L.K., 2004. Dynamic analysis of an arch due to a moving load. Journal of Sound and Vibration 269, 511–534.
Yang, Y.B., Wu, C.M., Yau, J.D., 2001. Dynamics response of a horizontally curved beam subjected to vertical and horizontal moving loads. Journal of Sound and Vibration 242 (3), 519–537.
Zhu, X.Q., Law, S.S., 2003. Dynamic behavior of orthotropic rectangular plates under moving loads. ASCE, Journal of Engineering Mechanics 129, 79–87.